Phenomenological model of Aluminum-hole defect formation in sedimentary quartz: Electron Spin Resonance (ESR) study

Khalif Benzid[1] and Alida Timar-Gabor[1,2*]

[1] Interdisciplinary Research Institute on Bio-Nano-Sciences, Babeş-Bolyai University, Cluj-Napoca, Romania.

[2] Faculty of Environmental Science and Engineering, Babeş-Bolyai University, Cluj-Napoca, Romania.

*alida.timar@ubbcluj.ro

Abstract

The mechanism governing the production of the paramagnetic Al-hole centres ($[AlO_4/h^+]^0$) in quartz as function of given dose is of great importance in Electron Spin Resonance (ESR) dating, as the analytical function used to characterise the evolution of this centre with accumulated dose is used to derive the equivalent dose by extrapolation to the abscissa-axis. The single saturating exponential model fails to accurately represent the dose response curve especially at high doses, and consequently, empirical functions, such as a saturating exponential plus a linear term, are widely used in the dating community. Herein, a physical phenomenological model is presented to describe the Al-hole formation under gamma irradiation in sedimentary quartz. We propose that Al-hole centre is formed via the dissociation of the Al centres compensated with alkali ions, generally denoted as $[AlO_4/M^+]^0$ where M^+ could be Li^+, Na^+ or K^+, as well as by the dissociation of Al compensated with hydrogen ($[AlO_4/H^+]^0$). We further assume then when irradiation moves alkali interstitials away from the aluminium ions, they can be replaced by H^+ ions beside the conversion to Al-hole centres. By assuming that the rate of the dissociation process is

proportional to the concentration of the defects themselves, a sum of saturating exponential functions is obtained for describing the growth of Al-hole with dose. Additionally, the model can be used also for predicting the evolution of the diamagnetic precursors ($[AlO_4/M^+]^0$ and $[AlO_4/H^+]^0$) with accumulated dose. The model is applied on data obtained on sedimentary quartz specimens of different origins for describing the dose response of the paramagnetic Al-hole ESR signal. We are showing that the signal of this later does not reach full saturation at doses even as high as 250 kGy and can be well represented by two exponential components as predicted by the model. As such, the additional linear term reported by other works when describing the dose response is but a first order approximation of one of the saturating exponential functions.

Key words: ESR dating, Al-hole centres ($[AlO_4/h^+]^0$), production mechanism, dose response curve.

Highlights

Physical model to describe the Al-hole production in quartz.

Irradiation in quartz moves alkali ions from aluminium ions and replaces them with protons or holes.

Al-hole forms by the dissociation of Al-M and Al-H.

Dose response curve of Al-hole in quartz is a sum of two saturating exponentials.

Dose response curve of Al-hole in quartz is not fully saturated even at 250 kGy.

1. Introduction

Trapped charge dating techniques such as Electron Spin Resonance (ESR) or luminescence methods are based on the assumption that the growth of the signals of interest in nature can be reproduced in the

laboratory by performing irradiations under controlled conditions. A dose response curve is constructed and the equivalent dose is determined by interpolation in the case of regenerative protocols or by extrapolation in the case of additive dose protocols. As such the selection of the function used to represent the dose response curve has a direct impact on the accuracy of the ages obtained.

Electron spin resonance measurements have the advantage of selectivity over luminescence methods, by which is meant that the signal used for dating is representing the signature of one single paramagnetic defect. Al-hole ($[AlO_4/h]^0$) signals in quartz have been extensively used for dating sediments (Duval et al., 2017; Duval and Guilarte, 2015; Laurent et al., 1998; Parés et al., 2018; Rink et al., 2007; Tissoux et al., 2012, 2008; Tsukamoto et al., 2018; Voinchet et al., 2004, 2013, 2019). Assuming a first order formation process of this defect, one would expect the dose response curve to be well represented by a single saturating exponential function. While in some studies a single saturating exponential function was used to fit the dose response curve of Al-hole signals (Laurent et al., 1998; Rink et al., 2007; Tissoux et al., 2008; Tsukamoto et al., 2018). It was later shown that such a model fails to accurately represent experimental data, especially in the high dose range (Grün, 1991; Duval, 2012). For this reason, other analytical functions, such as single saturating exponential plus a linear function (Duval et al., 2017; Parés et al., 2018; Voinchet et al., 2004, 2019) or a sum of two saturating exponentials (Tissoux et al., 2012) have been suggested to fit the growth of the ESR intensity of Al-hole with accumulated dose. The fact that the dose response curve cannot be generally well described by a single saturating exponential is an indication that the Al-hole centres formation can occur through more than one mechanism. Nevertheless, to our knowledge, no physical model has been proposed so far for explaining this dependence.

Trivalent aluminum ion is one of the most common substitutional impurities replacing silicon ion within the crystal lattice of quartz having an abundance ranging from a few tens to one thousand parts per

million in natural specimens (Preusser et al., 2009). The charge neutrality in quartz requires that the number of compensating cations, such as $^{7}Li^{+}$ (92.41% natural abundance), $^{23}Na^{+}$ (100% natural abundance) and $^{39}K^{+}$ (93.2% natural abundance) generally denoted by M^{+} and hydrogen $^{1}H^{+}$ should be similar to the number of Al^{3+} in Si^{4+} sites. In other words, aluminum is generally substitutional and compensated with interstitial cations (Weil, 1975). It has been shown that alkali, as well as hydrogen ions can be removed from Al sites when irradiation takes place at room temperature (Markes and Halliburton, 1979), consequently, forming the Al-hole paramagnetic centre ($[AlO_4/h]^0$). Likewise, it is known that irradiation leads to the dissociation of the $[AlO_4/M^+]^0$ centres and allows $[AlO_4/H^+]^0$ and $[AlO_4/h]^0$ centres to be formed. Simply stated, irradiation is carried out above 200 K interstitial alkali ions move away from the aluminium ions and are being replaced with protons or holes (Malik et al., 1981; Halliburton, 1989). The idea that holes replace the cations at aluminium sites was also exploited by other works (see the review of Preusser et al., 2009). Also, a reversible mechanism to that proposed above was presented in Mondragon et al., 1988 that proposed that hydrogen ions could replace holes, and thus decreasing Al-hole concentration at high doses.

Here we are presenting a phenomenological model that describes the evolution of the diamagnetic precursors ($[AlO_4/H^+]^0$ and $[AlO_4/M^+]^0$), as well as the production of Al-hole with accumulated gamma dose. We are further testing this model by fitting the dose response curves of Al-hole ESR signals for sedimentary quartz samples of various origins.

2. Samples and instrumentation

Sedimentary quartz samples from different locations that have been previously and securely dated by optically stimulated luminescence (OSL) are investigated. Sample END 1.2 is 63-90 μm quartz extracted

from Holocene soil at loess-paleosol sequence in Enders, Nebraska, Great Plains, USA. An equivalent dose of about 8 Gy was obtained for this samples using standard optically stimulated luminescence dating methods. Samples EVA 1098 and EVA 1095 are 125-212 μm quartz samples from Lake Durthong Australia, with OSL equivalent doses of about 72 Gy and about 12 Gy, respectively (Fitzsimmons, 2017). Rox Mix sample is 125-180 μm quartz originating from Roxolany loess paleosol sequence in Ukraine. Its OSL equivalent dose is about 15 Gy. More information on this sample can be found in (Anechitei-Deacu et al., 2018). The equivalent doses of the samples investigated here are thus negligible compared to the maximum doses given in our investigations (tens of kGy range).

Quartz has been extracted according to standard OSL preparation techniques, under subdued red light. The treatments included hydrochloric acid treatment to ensure carbonate removal, followed by hydrogen peroxide treatment for organic matter removal, sieving for selecting the desired grain size, density separation using heavy liquids (sodium metatungstate) and a final treatment with 40% hydrofluoric acid to assure feldspar removal, as well as for dissolving the outer surface of the grains.

Electron spin resonance analyses have been carried out using X band Bruker EMX plus spectrometer. Sample exposure to sunlight was restricted to minimum. The samples mass was approximately around 200 mg with variation of 5%. Irradiations have been performed at Centre for Nuclear Technologies, Technical University of Denmark (DTU NUTECH) using a calibrated ^{60}Co-60 gamma cell, with a dose rate of about 2 Gy/s (dose rate to water) at the time of irradiation. Dose rate to quartz was estimated to be 0.941 (with an uncertainty of 2.2% of the ratio) of dose rate to water based on Monte Carlo simulation considering the irradiation geometry used.

Parameters employed for recording Al-hole ESR signal were: temperature of 90 K, modulation frequency 100 kHz, modulation amplitude of 1 G, centerfield at 3350 G, sweep width of 300 G, 120s sweep time, 40 ms conversion time, 40.96 ms time constant, and microwave power of 2 mW. A single

scan was carried out and the average of two measurements was computed. ESR signal intensity of Al-hole was quantified as the peak to peak signal amplitude from g=2.018 to g=1.993 as recommended by (Toyoda and Falgueres, 2003)**.** Errors on the average ESR intensity have been computed according to (Toyoda and Falgueres, 2003).

3. Results and discussion

3.1 Phenomenological model of Al-hole formation

We consider an initial concentration of Al-hole (Al-h) formed previously by natural irradiation, denoted by N^0_{Al-h} and the initial concentrations of the diamagnetic precursors N^0_{Al-M} and N^0_{Al-} for $[AlO_4/M^+]^0$ and $[AlO_4/H^+]^0$ respectively. Laboratory irradiation transforms $[AlO_4/M^+]^0$ (Al-M) and $[AlO_4/H^+]^0$ (Al-H) into Al-h with certain rate constants, denoted here as λ_1 and λ_2, respectively. The direct transformation Al-H into Al-h is characterized by λ_3. This is schematically depicted in **figure 1**; the total amount of Al-h will be given by the sum of the concentration obtained via the process (i) and (ii) in addition to the initial concentration.

The only assumption made herein, is that the decay rate of precursor concentrations with dose, delivered with a constant dose rate is proportional to their own concentration.

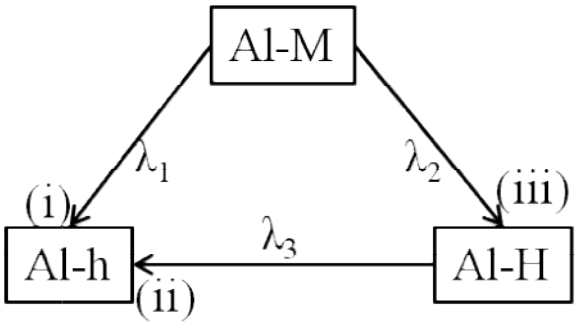

Figure 1: Schematic representation of Al-hole formation.

As such, one can write:

$$\frac{dN_{Al-M}}{dD} = -(\lambda_1 + \lambda_2)N_{Al-M} \quad (1)$$

Consequently the variation of Al-M with dose can be written as:

$$N_{Al-M} = N^0_{Al-M}\, e^{-(\lambda_1+\lambda_2)D} \quad (2)$$

The number of Al-h formed via process (i) can be written as:

$$N_{Al-h} = \frac{\lambda_1}{\lambda_1+\lambda_2} N^0_{Al-M} \left(1 - e^{-(\lambda_1+\lambda_2)D}\right) \quad (3)$$

The variation of Al-H as function of dose can be written as:

$$\frac{dN_{Al-H}}{dD} = \lambda_2\, N_{Al-M} - \lambda_3\ \ N_{Al-} \quad (4)$$

The first term of equation (4) gives the production of Al-H from the dissociation of Al-M while the second term depicts the simultaneous decrease of Al-H due to its transformation into Al-h. By introducing equation (2) into (4) and integrating, we get the dependence of Al-H with dose as:

$$N_{Al-H} = N^0_{Al-H}\, e^{-\lambda_3 D} + \frac{\lambda_2}{\lambda_1+\lambda_2-\lambda_3} N^0_{Al-M} \left(e^{-\lambda_3 D} - e^{-(\lambda_1+\lambda_2)D}\right) \quad (5)$$

The production of the Al-h from Al-H can be expressed as:

$$\frac{dN_{Al-h}}{dD} = -\lambda_3 N_{Al-H} \quad (6)$$

By introducing equation (5) into (6) and integrating, one obtains the variation of the produced Al-h via (ii) as:

$$N_{Al-h} = N^0_{Al-H}\left(1 - e^{-\lambda_3 D}\right) + \frac{\lambda_2}{\lambda_1+\lambda_2-\lambda_3} N^0_{Al-M} \left(\left(1 - e^{-\lambda_3 D}\right) - \frac{\lambda_3}{\lambda_1+\lambda_2}\left(1 - e^{-(\lambda_1+\lambda_2)D}\right)\right) \quad (7)$$

Consequently the total Al-h can be expressed as:

$$N_{Al-} = N_{Al-h}^{0} + \frac{\lambda_1}{\lambda_1+\lambda_2} N_{Al-M}^{0} \left(1 - e^{-(\lambda_1+\lambda_2)D}\right) + N_{Al-H}^{0} \left(1 - e^{-\lambda_3 D}\right) + \frac{\lambda_2}{\lambda_1+\lambda_2-\lambda_3} N_{Al-M}^{0} \left(\left(1 - e^{-\lambda_3 D}\right) - \frac{\lambda_3}{\lambda_1+\lambda_2}\left(1 - e^{-(\lambda_1+\lambda_2)D}\right)\right) \quad (8)$$

Where N_{Al-h}^{0} is a constant representing in this case the initial concentration of Al-h existing in the sample before laboratory irradiation.

There are two main terms; the first one gives the amount of Al-h produced directly from Al-M (i), while the second term which is itself the sum of two exponentials depicts the formation via processes characterised by λ_2 and λ_3 (ii) and (iii), respectively. For this second term the first exponential is the Al-h formed from the initial concentration of Al-H while the last term represents the Al-h formed from Al-M via the transformation of Al-H.

Equation (8) gives the increase of Al-h with dose and can also be simplified as the sum of two saturating exponentials:

$$N_{Al-h} = N_{Al-h}^{0} + A_1\left(1 - e^{-(\lambda_1+\lambda_2)D}\right) + A_2\left(1 - e^{-\lambda_3 D}\right) \quad (9)$$

where $A_1 = \frac{\lambda_1-\lambda_3}{\lambda_1+\lambda_2-\lambda_3} N_{Al-M}^{0}$ and $A_2 = \frac{N_{Al-H}^{0}(\lambda_1+\lambda_2-\lambda_3)+\lambda_2 N_{Al-M}^{0}}{\lambda_1+\lambda_2-\lambda_3}$

Considering equations (8) and (9), when λ_2 tends to 0 we will have $A_1 = N_{Al-M}^{0}$ and $A_2 = N_{Al-H}^{0}$,

as such the process can be seen as the sum of two independent exponential processes. However, if $\lambda_3 = \lambda_1 + \lambda_2 = \lambda$ the Eq. (9) becomes a single saturation exponential:

$$N_{Al-h} = N_{Al-h}^{0} + (N_{Al-H}^{0} + N_{Al-M}^{0})\left(1 - e^{-\lambda D}\right) \quad (10)$$

Besides, if one of the processes is negligible relatively to the second process, $\lambda_3 \gg \lambda_1 + \lambda_2$ or vice-versa, one exponential will dominate the second and only one process remains significant in the dose response curve.

When we consider only the first order development of one of the exponential functions, one can obtain the exponential plus linear dependence as following:

$$N_{Al-h} = N^0_{Al-h} + A_1\left(1 - e^{-(\lambda_1+\lambda_2)D}\right) + A_2\lambda_3 D \quad (11)$$

The second term herein is only a first order approximation of one of the process. This explains why functions such as an exponential plus a linear term (eq. 11) can fit well the dose response curve in a certain restricted dose range as reported by others (see Duval, 2012 and references therein).

3.2. Dose response curves for natural samples

A typical Al-hole ESR signal is presented in **figure 2**. To constrain the behavior of this signal for very high doses, dose response curves have been constructed up to 250 kGy for two samples, where enough material was available. These dose response curves, constructed using the standard multiple added dose protocol are presented in **figure 3**. It can be clearly noticed that the signal dose not reach full saturation in the up to tens of kGy dose range usually employed in typical ESR dating studies.

The dose response curves presented in **figure 3** were fitted using equation (8) and the parameters are presented in **table 1**, along with the parameters obtained for fitting the dose response curves recorded for sedimentary quartz samples END 1.2. and ROX mix. For these samples, the dose response curves were constructed up to maximum doses of 40 kGy due to the limited availability of material.

For fitting, no special constrains have been employed. However, we considered two scenarios; in the first scenario, the initial concentration of Al-M is larger than that of Al-H, while in the second assumption, we considered a larger initial concentration of Al-H than that of Al-M. Given the variability of the concentration of Al-hole precursors in different natural quartz specimens, both assumptions are

reasonable. To our knowledge, there is yet no quantitative information available that could point out towards which of the two possibilities is to be preferred.

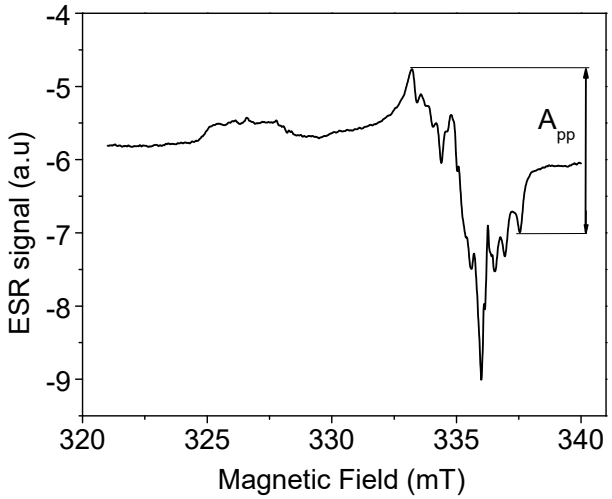

Figure 2: ESR spectrum recorded at 90K with 2mW of microwave power and 9417.55 MHz. The amplitude peak to peak (App) of the Al-hole signal is indicated according to Toyoda and Falgueres 2003.

Table 1: Parameters obtained by fitting the dose response curves recorded for Al-hole signal. The first list of parameters presented for each sample corresponds to the assumption that the initial concentration of Al-M is larger than that of Al-H. The values presented in italic correspond to the opposite assumption, namely that the concentration of Al-H is the majority. For samples and data indicated by a star (*) values up to 250 kGy were used to construct the dose response curve. All the other values correspond to dose response curves constructed up to doses as high as 40 kGy (E-x=10^{-x}).

	N^0_{Al-M}	N^0_{Al-H}	λ_1	λ_2	λ_3	N^0_{Al-h}	R^2
END 1.2	7.9	1.9	2.3E-5	2.3E-5	0.0035	2.2	0.995
END 1.2	*1.86*	*7.78*	*0.0034*	*1.43E-4*	*4.6E-5*	*2.2*	*0.995*
EVA 1098	12.0	2.2	3E-5	1.3E-5	0.001	0.86	0.999
EVA 1098	*2.11*	*11.94*	*9.7E-4*	*5.6E-5*	*4.42E-5*	*0.86*	*0.999*
EVA 1098*	13.12	3.04	1.03E-4	7.36E-5	1.36E-5	0.86	0.99

EVA 1098*	*7.37*	*8.76*	*1.7E-4*	*2.7E-6*	*1.35E-5*	*0.86*	*0.99*
EVA 1095	15.91	4.65	8.7E-6	1.08E-5	3.1E-4	1.37	0.997
EVA 1095	*4.64*	*15.91*	*2.7E-4*	*3.66E-5*	*1.95E-5*	*1.37*	*0.997*
EVA 1095*	13.7	3.9	1.57E-5	1.19E-5	3.6E-4	1.37	0.998
EVA 1095*	*6.65*	*10.97*	*2E-4*	*1.62E-4*	*2.76E-5*	*1.37*	*0.998*
ROX Mix	3.2	0.76	1.08E-5	3.1E-5	0.002	0.96	0.997
ROX Mix	*0.8*	*3.2*	*0.00145*	*2.46E-4*	*4.03E-5*	*0.96*	*0.997*

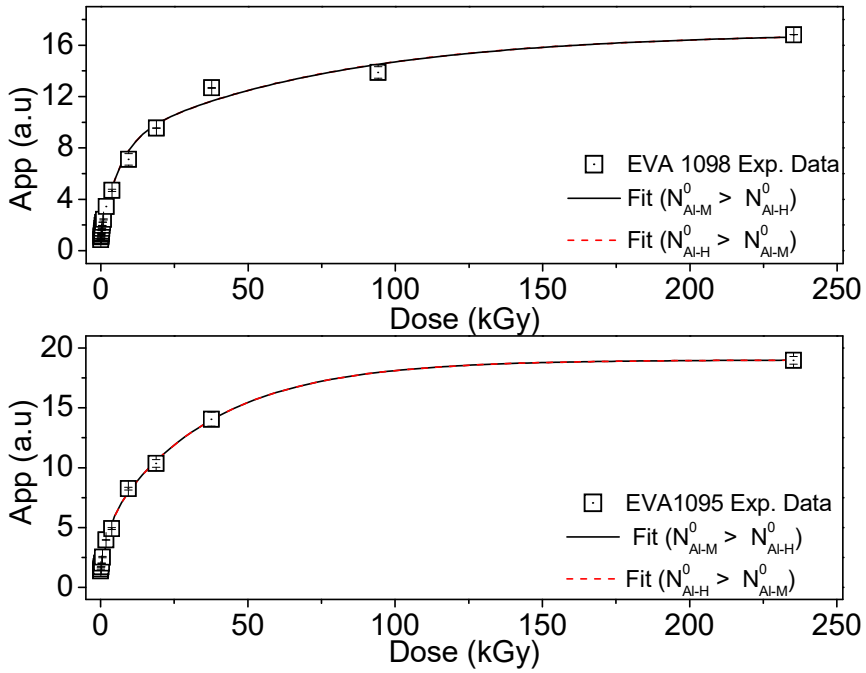

Figure 3: Dose response of Al-h centre constructed up to 250 kGy for EVA 1098 and EVA 1095.

We acknowledge the hazards of interpreting the parameters derived through fitting with multiple exponentials, especially as the amplitudes of the two exponentials (A_1 and A_2 in eq. 9) depend on both the initial concentrations of the precursors, as well as the rate constants of different mechanisms. However, for a sum of exponentials used for fitting, if the parameters obtained for the fit that characterise the process are significantly different, it is unlikely that these components could be fitting artifacts (Istratov and Vyvenko, 1999). From **table 1,** it can be seen that this condition is mostly fulfilled

for investigated samples. When analysing dose response curves obtained for optically stimulated luminescence signals fitted with a sum of two saturating exponential functions, we have previously shown that the parameters obtained depend on the maximum given dose, unless the dose response is constructed to high enough doses in order to reach full saturation (Timar-Gabor et al., 2017). As such, if one wants to make quantitative assumptions using the derived parameters, the dose response curve needs to be raised until full saturation. This is difficult as we have shown that the signal is not in full saturation for doses even as high as 250 kGy (**figure 3**). Due to this reason, in order to allow the comparison of the obtained parameters from one sample to another, here, we are presenting the parameters obtained for all samples for dose response curves up to 40 kGy. For the sake of rigor, we are likewise presenting the parameters obtained for the dose response curves measured up to doses of 250 kGy for EVA samples, as we consider these parameters to be more reliable.

The actual dose response curves constructed up to 40 kGy and fitted using equation (8) are presented in **figure 4.** The scenario where the initial Al-M concentration dominates the initial Al-H concentration is depicted in the left hand figure, while the right hand diagrams are based on the assumption that at the beginning of irradiation there is a higher concentration of Al-H than that of Al-M. The Al-h produced via the two processes described in the model, namely from the direct disintegration of Al-M through (i) (first term in eq. 8) or via the mechanism (ii), involving the replacement of alkali with hydrogen ions (second terms in eq. 8) are presented separately (**figure 4**). One can note that when the initial concentration of Al-M is higher than the initial concentration of Al-H the concentration of Al-hole obtained by the two processes seems to not tend to be saturated, at least in this dose range. However, if the initial concentration of Al-H is larger than that of Al-M, the process denoted as (i) (**figure 1**) is fully saturated before process (ii).

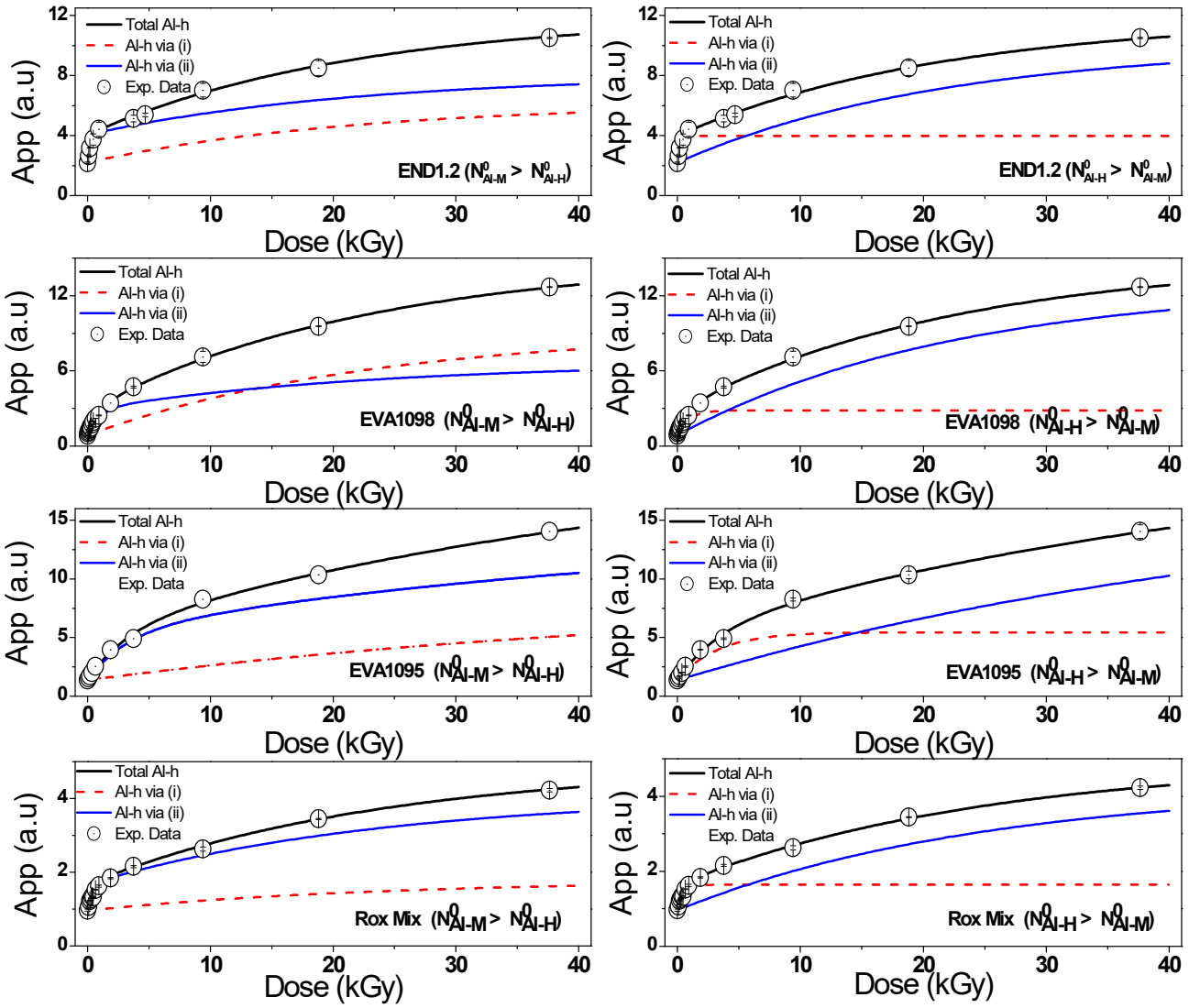

Figure 4: Dose response curves recorded up to 40 kGy for the investigated samples fitted (black continuous line) using equation (8). The behavior (based on the fitting parameters) of the Al-h produced via process (i) and (ii) is presented as a dashed red line and as continuous blue line, respectively. The case of Al-M > Al-H is presented in the left hand panels while the case of Al-H > Al-M is shown in the right hand panels. Please note that in the case of samples EVA 1098 and EVA 1095 the data represents the same values as presented in figure 3, but neglecting the very high dose points (100 kGy and 250 kGy)

Based on the parameters obtained (**table 1**), equations (2) and (5) allow one to predict the evolution of Al-M and Al-H respectively, as well as the evolution of their sum, with dose. Furthermore, performing some independent measurements that could monitor the evolution of the diamagnetic Al-H defects with dose, in particular, and Al-M defects in general, the presented model should contribute to a deeper understanding of these defects dynamics in quartz during irradiation. The process rate parameters (λ_i), as well as the initial concentrations that can be obtained by applying this model allows deriving information on the rate of releasing alkali ions as function of dose. Even more, one could get information on how the simultaneous processes of dissociation and formation of Al-H, via processes denoted as (ii) and (iii) respectively, result in hydrogen ions being released and/or captured by other adjacent defects as function of given dose. This is important information, as besides electronic processes, ionic processes have been proposed a few decades ago for explaining defect dynamics upon irradiation and stimulation in quartz (Itoh et al., 2002) and currently they are being used for explaining different mechanisms in quartz such as bleaching of optically stimulated luminescence signals (Williams et al., 2018) or thermoluminescence emission spectra (Williams and Spooner, 2018).

4. Summary

Al-hole paramagnetic signal is often used in Electron Spin Resonance dating of quartz. While it is well known that the dose response of this signal cannot be well represented by a single saturating exponential function, no model has yet been presented. Here, we propose a physical model for explaining the growth of Al-hole paramagnetic centres with dose in quartz. Based on other works, we are suggesting that this centre is formed via the dissociation of substitutional Al compensated by alkali and hydrogen ions under gamma irradiation, followed by trapping holes. In addition, we are making an allowance for the possibility that when alkali ions are removed, they can be replaced by hydrogen ions as well as by holes.

By assuming that the dissociation rates of these centres are proportional to their concentrations, the model shows that the increase of Al-hole ESR signal with dose can be well described by a sum of two exponential functions. The model accurately describes the dose response curves recorded for natural sedimentary quartz samples of various origins and will hopefully contribute obtaining more accurate equivalent doses in ESR dating. Moreover, if it would be complemented by the simultaneous monitoring of the behavior of Al-hole precursors in quartz, the presented model could contribute to further understanding on these defects dynamics upon irradiation.

Acknowledgements:

This project received funding from the European Research Council (ERC) under the European Union's Horizon 2020 research and innovation programme ERC-2015-STG (grant agreement No [678106]). K. Fitzsimmons from Research Group for Terrestrial Palaeoclimates, Max Planck Institute for Chemistry, Mainz, Germany is highly acknowledges for providing us the EVA samples. M. Bailey from Risø High Dose Reference Laboratory, Technical University of Denmark is thanked for carrying out the gamma irradiations. Viorica Tecșa is thanked for carrying out the sample preparation of END sample.

References

Anechitei-Deacu, V., Timar-Gabor, A., Thomsen, K.J., Buylaert, J.-P., Jain, M., Bailey, M., Murray, A.S., 2018. Single and multi-grain OSL investigations in the high dose range using coarse quartz. Radiat. Meas., 120, 124–130. https://doi.org/10.1016/j.radmeas.2018.06.008

Duval, M., 2012. Dose response curve of the ESR signal of the Aluminum centre in quartz grains extracted from sediment. Ancient TL 30, 31-45.

Duval, M., Arnold, L.J., Guilarte, V., Demuro, M., Santonja, M., Pérez-González, A., 2017. Electron spin resonance dating of optically bleached quartz grains from the Middle Palaeolithic site of

Cuesta de la Bajada (Spain) using the multiple centres approach. Quat. Geochronol. 37, 82–96. https://doi.org/10.1016/j.quageo.2016.09.006

Duval, M., Guilarte, V., 2015. ESR dosimetry of optically bleached quartz grains extracted from Plio-Quaternary sediment: Evaluating some key aspects of the ESR signals associated to the Ti-centres. Radiat. Meas. 78, 28–41. https://doi.org/10.1016/j.radmeas.2014.10.002

Fitzsimmons, K.E., 2017. Reconstructing palaeoenvironments on desert margins: New perspectives from Eurasian loess and Australian dry lake shorelines. Quat. Sci. Rev. 171, 1–19. https://doi.org/10.1016/j.quascirev.2017.05.018

Grün, R., 1991. Potential and problems of ESR dating. Int. J. Radiat. Appl. Instrum. Part Nucl. Tracks Radiat. Meas. 18, 143–153. https://doi.org/10.1016/1359-0189(91)90106-R

Halliburton, L.E., 1989. ESR and optical characterization of point defects in quartz. Int. J. Rad. Appl. Instrum. [A] 40, 859–863. https://doi.org/10.1016/0883-2889(89)90007-5

Istratov, A.A., Vyvenko, O.F., 1999. Exponential analysis in physical phenomena. Rev. Sci. Instrum. 70, 1233–1257. https://doi.org/10.1063/1.1149581

Itoh, N., Stoneham, D., Stoneham, A.M., 2002. Ionic and electronic processes in quartz:Mechanisms of thermoluminescence and optically stimulated luminescence. J. Appl. Phys. 92, 5036–5044. https://doi.org/10.1063/1.1510951

Laurent, M., Falguères, C., Bahain, J.., Rousseau, L., Van Vliet Lanoé, B., 1998. ESR dating of quartz extracted from quaternary and neogene sedimentsmethod, potential and actual limits. Quat. Sci. Rev. 17, 1057–1062. https://doi.org/10.1016/S0277-3791(97)00101-7

Malik, D.M., Kohnke, E.E., Sibley, W.A., 1981. Low-temperature thermally stimulated luminescence of high quality quartz. J. Appl. Phys. 52, 3600–3605. https://doi.org/10.1063/1.329092

Markes, M.E., Halliburton, L.E., 1979. Defects in synthetic quartz: Radiation-induced mobility of interstitial ions. J. Appl. Phys. 50, 8172–8180. https://doi.org/10.1063/1.325957

Mondragon, M.A., Chen, C.Y., Halliburton, L.E., 1988. Observation of a doserate dependence in the production of point defects in quartz. J. Appl. Phys 63, 4937-4941. https://doi.org/10.1063/1.341156

Parés, J.M., Álvarez, C., Sier, M., Moreno, D., Duval, M., Woodhead, J.D., Ortega, A.I., Campaña, I., Rosell, J., Bermúdez de Castro, J.M., Carbonell, E., 2018. Chronology of the cave interior sediments at Gran Dolina archaeological site, Atapuerca (Spain). Quat. Sci. Rev. 186, 1–16. https://doi.org/10.1016/j.quascirev.2018.02.004

Preusser, F., Chithambo, M.L., Götte, T., Martini, M., Ramseyer, K., Sendezera, E.J., Susino, G.J., Wintle, A.G., 2009. Quartz as a natural luminescence dosimeter. Earth-Sci. Rev. 97, 184–214. https://doi.org/10.1016/j.earscirev.2009.09.006

Rink, W.J., Bartoll, J., Schwarcz, H.P., Shane, P., Bar-Yosef, O., 2007. Testing the reliability of ESR dating of optically exposed buried quartz sediments. Radiat. Meas. 42, 1618–1626. https://doi.org/10.1016/j.radmeas.2007.09.005

Toyoda, S. and Falgueres, C., 2003.The method to represent the ESR signal intensity of the aluminum hole centre in quartz for the purpose of dating. Advances in ESR Applications, 20, 7-10., n.d.

Timar-Gabor, A., Buylaert, J.-P., Guralnik, B., Trandafir-Antohi, O., Constantin, D., Anechitei-Deacu, V., Jain, M., Murray, A.S., Porat, N., Hao, Q., Wintle, A.G., 2017. On the importance of grain size in luminescence dating using quartz. Radiat. Meas. 106, 464–471. https://doi.org/10.1016/j.radmeas.2017.01.009

Tissoux, H., Toyoda, S., Falguères, C., Voinchet, P., Takada, M., Bahain, J.-J., Despriée, J., 2008. ESR Dating of Sedimentary Quartz from Two Pleistocene Deposits Using Al and Ti-Centres. Geochronometria 30, 23–31. https://doi.org/10.2478/v10003-008-0004-y

Tissoux, H., Voinchet, P., Lacquement, F., Prognon, F., Moreno, D., Falguères, C., Bahain, J.-J., Toyoda, S., 2012. Investigation on non-optically bleachable components of ESR aluminium signal in quartz. Radiat. Meas. 47, 894–899. https://doi.org/10.1016/j.radmeas.2012.03.012

Tsukamoto, S., Long, H., Richter, M., Li, Y., King, G.E., He, Z., Yang, L., Zhang, J., Lambert, R., 2018. Quartz natural and laboratory ESR dose response curves: A first attempt from Chinese loess. Radiat. Meas. 120, 137–142. https://doi.org/10.1016/j.radmeas.2018.09.008

Voinchet, P., Bahain, J.J., Falguères, C., Laurent, M., Dolo, J.M., Despriée, J., Gageonnet, R., Chaussé, C., 2004. ESR dating of quartz extracted from Quaternary sediments application to fluvial terraces system of northern France [Datation par résonance paramagnétique électronique (RPE) de quartz fluviatiles quaternaires: application aux systèmes de terrasses du nord de la France.]. Quaternaire 15, 135–141. https://doi.org/10.3406/quate.2004.1761

Voinchet, P., Yin, G., Falguères, C., Liu, C., Han, F., Sun, X., Bahain, J., 2013. ESR dose response of Al centre measured in quartz samples from the Yellow River (China): Implications for the dating of Upper Pleistocene sediment. Geochronometria 40, 341–347. https://doi.org/10.2478/s13386-013-0131-8

Voinchet, P., Yin, G., Falguères, C., Liu, C., Han, F., Sun, X., Bahain, J.-J., 2019. Dating of the stepped quaternary fluvial terrace system of the Yellow River by electron spin resonance (ESR). Quat. Geochronol. 49, 278–282. https://doi.org/10.1016/j.quageo.2018.08.001

Weil, J.A., 1975. The aluminum centers in α-quartz. Radiat. Eff. 26, 261–265. https://doi.org/10.1080/00337577508232999

Williams, O.M., Spooner, N.A., 2018. Defect pair mechanism for quartz intermediate temperature thermoluminescence bands. Radiat. Meas. 108, 41–44. https://doi.org/10.1016/j.radmeas.2017.11.005

Williams, O.M., Spooner, N.A., Smith, B.W., Moffatt, J.E., 2018. Extended duration optically stimulated luminescence in quartz. Radiat. Meas. 119, 42–51. https://doi.org/10.1016/j.radmeas.2018.09.005